

In Situ X-ray Diffraction during Forced Silking of Spider Silk

Christian Riekkel* and Martin Müller

European Synchrotron Radiation Facility, B.P. 220,
F-38043 Grenoble Cedex, France

Fritz Vollrath

Department of Zoology, University of Aarhus,
Universitetsparken B135, DK 8000, Aarhus C, Denmark

Received January 20, 1999

Introduction. As the result of an evolutionary process,¹ dragline spider silk combines high elasticity with high strength² and the ability to quickly modify fibers to suit the task at hand.³ It is assumed that feedstock and spinning conditions interact to produce the final thread⁴ and, furthermore, that threads with different mechanical properties differ in microstructure.⁵ In situ X-ray diffraction experiments during extrusion of synthetic polymers allows correlating processing parameters with the structural properties.⁶ The exceedingly low mass of silk produced by a spider has, however, not allowed investigating in a similar way of the extrusion of this biopolymer. In the present communication, we will show that such experiments have become possible by using an X-ray microbeam.

Experimental Section. Sample Preparation. The forced silking technique⁷ was used to extract major ampullata silk from a *Nephila senigalensis* spider. The spider was first anesthetized with CO₂ and then fixed with its ventral side up on a metal support using soft tape. Specimen and holder were transferred to the X-ray microbeam setup, which is shown in Figure 1. During the diffraction experiments, the spider was awake. A single fiber was horizontally pulled out from one of the spigots onto a motor-driven take-up spool. Extraction continued for about 8 h at reeling speeds between 0.2 and 0.9 cm s⁻¹. The diameter of the fiber was determined by scanning electron microscopy (SEM) as 3.7 μm on the last part of the fiber pulled out at 0.2 cm s⁻¹.

X-ray Diffraction. An X-ray beam with a 0.0782 nm wavelength and a 7 μm spot size (full width at half-maximum, fwhm) from the microfocus beamline at the European Synchrotron Radiation Facility was used.⁸ The sample environment was kept at 25.5 ± 0.5 °C with lights switched off during data collection. Lights were, however, switched on when changing the reeling speed. The spider and its support structure were placed on a three-axis gantry, which was interfaced to a computer-controlled motion software. This allowed for the transference of a specific point on the fiber from the focal point of an optical microscope into the X-ray beam. Optical measurements showed that the position of the fiber in the beam was constant to at least the X-ray beam size. The length of the fiber from the exit of the spigot to the X-ray beam was chosen to be about 10 mm. During data collection the fiber was moved vertically through the X-ray beam with 4 μm steps as it was pulled out from the spigot and diffraction patterns of 180 s each

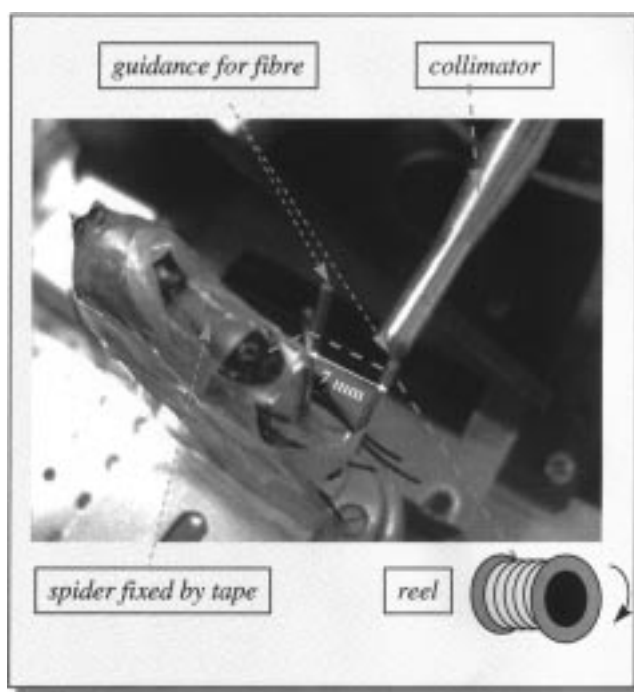


Figure 1. Experimental setup for in situ diffraction during forced silking. The spider is fixed by soft tape to a support, leaving head, breathing duct, and spigots free. The path of the fiber to the motorized reel is schematically indicated. The collimator serves to define the X-ray beam and in particular reduce background scattering. Beamstop and 2D-CCD detector are not shown.

were recorded at every position by a MAR CCD-detector. For analysis the pattern with the strongest diffraction pattern within each scan was used. Background correction was performed with a pattern recorded in the same sequence where the beam was just outside the fiber. Al₂O₃ powder was used for instrumental calibration.

Results and Discussion. Diffraction patterns recorded at all reeling speeds are very similar and show a semicrystalline morphology which is characterized by Bragg reflections, an oriented amorphous halo, and a diffuse halo (Figure 2a). The patterns agree with the model of small crystalline blocks in a matrix containing both oriented and unoriented amorphous material.^{9,10} A fiber from the same specimen, stored in air for about one month before data collection, shows the same structural features as the fresh fiber with an additional meridional superlattice reflection (Figure 2b). The crystalline fraction corresponds to the pattern of the β-poly-(L-alanine) structure.¹¹ For indexation, a unit cell with double *a*-axis was chosen to keep the original cell geometry of Warwicker (basic lattice, BL).¹² Figure 3 shows a fit of a series of Gaussian functions to the azimuthal intensity profile centered on the superlattice reflection. The meridional superlattice reflection of the stored sample (lattice spacing: *d* = 0.420 nm) cannot be indexed with a *c*-axis (fiber axis) of ~0.7 nm although it appears to belong to the (00*l*)-series as its azimuthal width of 19.5° (fwhm) corresponds to the width of the (002) reflection. A possible explanation for the appearance of a superlattice reflection would be a tripling of the *c*-axis due to a repeating motif of three amino acids,

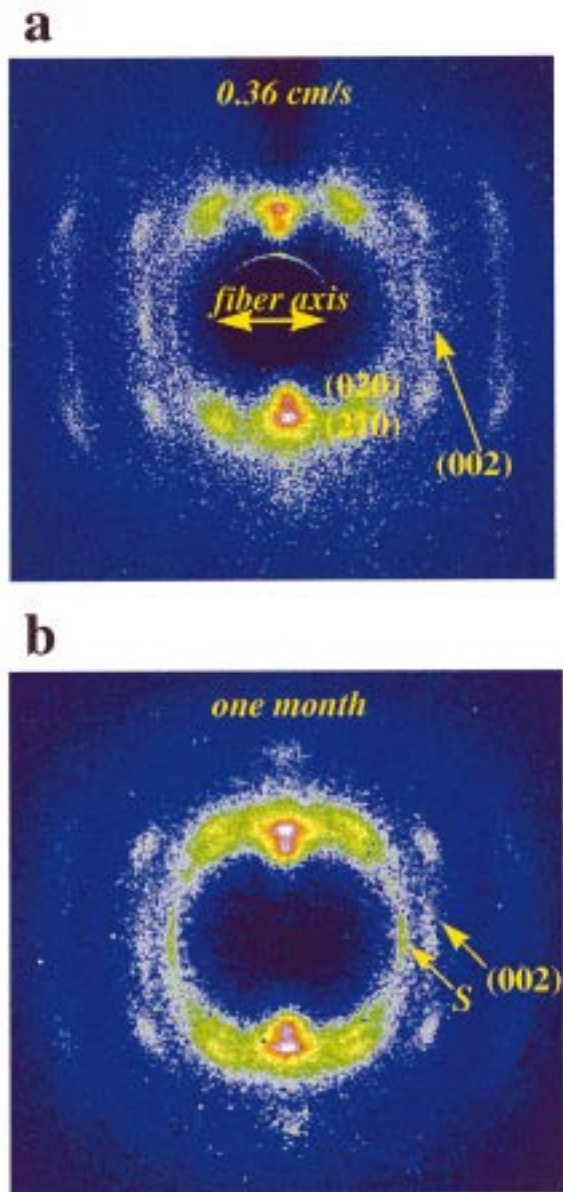


Figure 2. (a) X-ray diffraction pattern of *N. senigalensis* fiber recorded at a reeling speed of 0.36 cm s^{-1} . (b) Diffraction pattern obtained from same species after about one month aging of the fiber. The pattern has been scaled differently than that in part a to enhance the visibility of the meridional superlattice reflection (S). Lattice spacing of strongest reflections: (020), $d = 0.54 \text{ nm}$; (210), $d = 0.44 \text{ nm}$; (002), $d = 0.348 \text{ nm}$; superlattice reflection S, $d = 0.420 \text{ nm}$.

–GGX–, where G corresponds to glycine and X to larger amino acids such as serine, as proposed for *N. clavipes*.¹³ The superlattice reflection could then be indexed as (005). Meridional reflections with $l = 2n + 1$ indices have not yet been observed for *N. clavipes* silk by X-ray diffraction^{10,14,15} but have been observed by electron diffraction.¹³ No evidence for additional equatorial reflections was, however, obtained.¹⁶ The model suggested above implies a structural flexibility in the solid state which results in changes of the long-range order due to a slow incorporation of glycine-containing sequences into the crystalline blocks composed principally of polyaniline chain segments. This observation suggests that crystallinity estimations based only on the assumption of crystalline polyaniline blocks¹⁰ are too low.

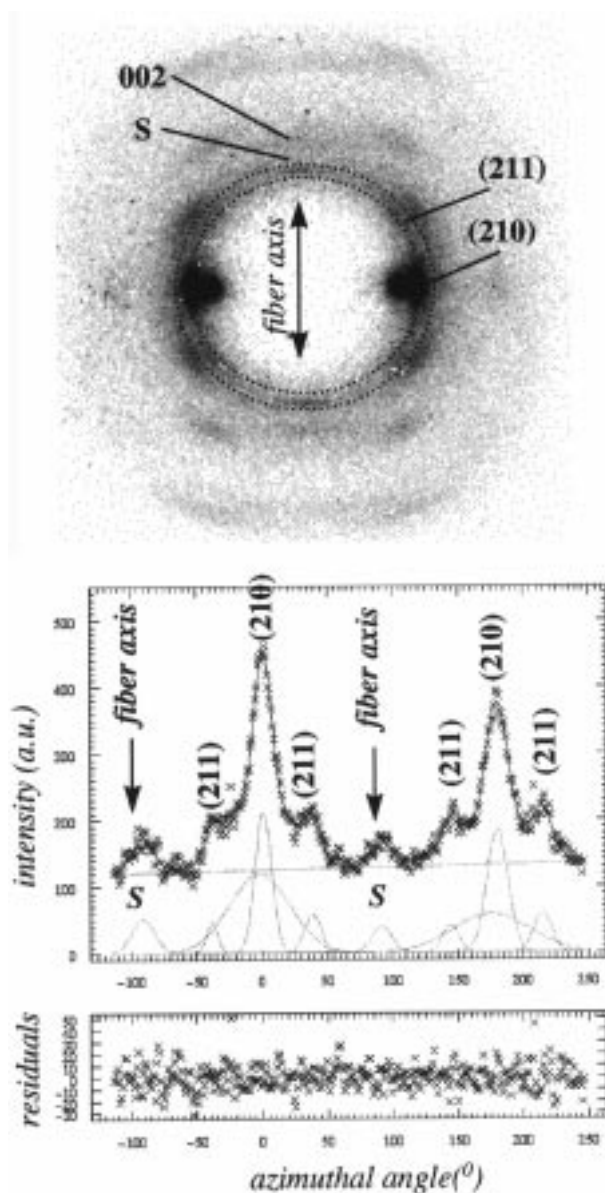


Figure 3. Extraction of azimuthal intensity distribution from an annulus centered on the superlattice reflection (top). The profile can be simulated by a series of Gaussian functions (bottom). Note the broad Gaussian profile below the (210) reflection due to the oriented halo.

Radial profiles of equatorial reflections can be separated into Gaussian profiles of different width due to the crystalline blocks and the oriented amorphous halo.^{10,16} Figure 4a,b shows the variation of lattice spacing, d , and the average particle size, L , (calculated from the Scherrer equation) for the (020) and (210) reflections. L -values along the a - and b -directions of the lattice are 2–3 nm, which is similar to a *N. clavipes* fiber bundle.¹⁰ The variation of reeling speed apparently does not influence the lateral packing of the chains and the size of the crystallites. This also holds for the BL (002) meridional reflection and hence the size of the blocks along the fiber axis ($L = 7 \text{ nm}$). Whether this also holds for the speeds up to 10 cm s^{-1} that spiders are capable of spinning will have to be further investigated. For the present reeling speeds one can determine an average BL-unit cell from the (210)/(020) and the (002) reflections with $a = 0.97(1)$, $b = 1.09(1)$, and $c = 0.697(3) \text{ nm}$.

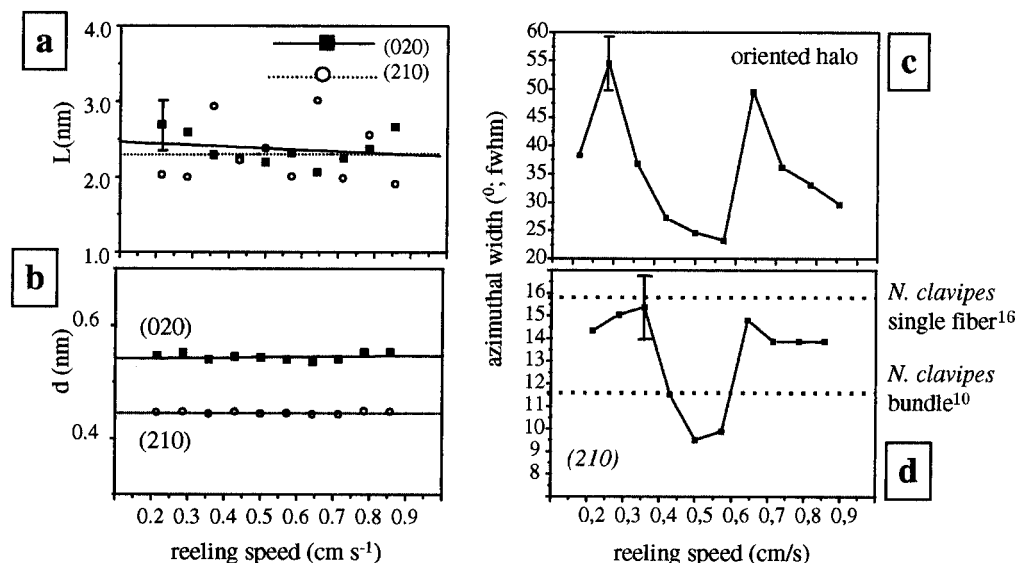


Figure 4. (a) Variation of apparent particle size, L (nm), and (b) lattice spacing, d (nm), of (020) and (210) reflections as a function of reeling speed. The lines are polynomial (first-order) fits. The slight slope of the $L(020)$ fit is statistically not significant. The error bars in part b correspond to the size of the squares. (c) Variation of oriented halo and (d) azimuthal width of (210) reflection as a function of reeling speed. Reference values were determined under static conditions from *N. clavipes* silk for a single fiber obtained from a freely foraging spider¹⁶ and a fiber bundle collected during forced silking at 2 cm/s.¹⁰ Line connecting experimental points serves as guide lines for the eye.

Orientation in polymers is related to mechanical anisotropy.¹⁷ Stretching of *N. clavipes* fibers results in an improved alignment of anisotropic crystalline blocks,¹⁰ which can be expressed in terms of an average angle of the normal to the (00 l) planes and hence molecular chains along the fiber axis: $\langle \cos^2 \phi_f \rangle$.¹⁷ As the pulling speed appears to modify the mechanical properties of spider silk,¹⁸ we expect a variation of this average angle. $\langle \cos^2 \phi_f \rangle$ can be derived from the azimuthal width of the two strongest equatorial reflections: (210)/(020).^{17,10} We find a variation of azimuthal width of the (210) reflection with reeling speed (Figure 4d) which suggest hence a variation of $\langle \cos^2 \phi_f \rangle$ and therefore of the microstructure. The bandwidth of this variation corresponds approximately to values obtained for a *N. clavipes* fiber bundle collected at a reeling speed of 2 cm/s¹⁰ and a single fiber of silk collected from a freely foraging spider.¹⁶ The azimuthal width of the oriented amorphous component shows a similar variation (Figure 4c). Given the possible incorporation of -GGX- sequences into the crystalline blocks, it is probable that the overall crystallinity of *Nephila* silk is higher than the about 12% value obtained by X-ray diffraction and closer to about 50%, derived from molecular modeling of the mechanical properties;¹⁹ it is therefore tempting to relate the oriented phase to the proposed, about 5 nm thick interface that is assumed to exist around the crystalline blocks.¹⁹ It is quite possible that the modulation in orientation is induced through a mechanical action on the exit of the spigot which is subject to the state of the spider. The experimental method presented in this communication will allow studying this topic in more detail.

References and Notes

- (1) Selden, P. A. *Nature* **1989**, *340*, 711–713.
- (2) Gosline, J. M.; DeMont, M. E.; Denny, M. W. *Endeavour* **1986**, *10*, 37–43.
- (3) Vollrath, F.; Köhler, T. *Proc. R. Soc. London* **1996**, *263*, 387–391.
- (4) Kaplan, D.; Adams, W. W.; Farmer, B.; Viney, C. *Silk Polymers: Materials Science and Biotechnology*; Kaplan, D., Adams, W. W., Farmer, B., Viney, C., Ed.; American Chemical Society: Washington, 1994; Vol. 544.
- (5) Guess, K. B.; Viney, C. *Thermochim. Acta* **1998**, *315*, 61–66.
- (6) Cakmak, M.; Teitge, A.; Zachmann, H. G.; White, J. L. *J. Polym. Sci.* **1993**, *B31*, 371–381.
- (7) Work, R. W.; Emerson, P. D. *J. Arachnol.* **1982**, *10*, 1–10.
- (8) Riekel, C.; Cedola, A.; Heidelberg, F.; Wagner, K. *Macromolecules* **1997**, *30*, 1033–1037.
- (9) Simmons, A. H.; Michal, C. A.; Jelinski, L. W. *Science* **1996**, *271*, 84–87.
- (10) Grubb, D. T.; Jelinski, L. W. *Macromolecules* **1997**, *30*, 2860–2867.
- (11) Arnott, S.; Dover, S. D.; Elliott, A. *J. Mol. Biol.* **1967**, *30*, 201–208.
- (12) Warwicker, J. O. *J. Mol. Biol.* **1960**, *2*, 350–362.
- (13) Thiel, B. L.; Kunkel, D. D.; Viney, C. *Biopolymers* **1994**, *34*, 1089–1097.
- (14) Parkhe, A. D.; Seeley, S. K.; Gardner, K.; Thompson, L.; Lewis, R. V. *J. Mol. Recognit.* **1997**, *10*, 1–6.
- (15) Bram, A.; Bränden, C. I.; Craig, C.; Snigireva, I.; Riekel, C. *J. Appl. Crystallogr.* **1997**, *30*, 390–392.
- (16) Riekel, C.; Bränden, C.; Craig, C.; Ferrero, C.; Heidelberg, F.; Müller, M. *Int. J. Mol. Biol.* **1999**, *24* (2–3), 179–186.
- (17) Ward, I. M. *Structure and Properties of Oriented Polymers*; Ward, I. M., Ed.; Applied Science Publishers: London, 1975.
- (18) Madsen, B.; Shao, Z. Z.; Vollrath, F. *Int. J. Mol. Biol.* **1999**, *24* (2–3), 301–306.
- (19) Termonia, Y. *Macromolecules* **1994**, *27*, 7378–7381.

MA990067A